HHS Public Access

Author manuscript

Nat Neurosci. Author manuscript; available in PMC 2020 January 09.

Published in final edited form as:

Nat Neurosci. 2018 June ; 21(6): 803–807. doi:10.1038/s41593-018-0151-z.

Chronic CRH depletion from GABAergic, long-range projection neurons in the extended amygdala reduces dopamine release and increases anxiety

Nina Dedic[1,9], **Claudia Kühne**[1,9], **Mira Jakovcevski**[1], **Jakob Hartmann**[1,2], **Andreas J. Genewsky**[1], **Karina S. Gomes**[1,3], **Elmira Anderzhanova**[1], **Max L. Pöhlmann**[1], **Simon Chang**[1], **Adam Kolarz**[1], **Annette M. Vogl**[1], **Julien Dine**[1], **Michael W. Metzger**[1], **Bianca Schmid**[1], **Rafael C. Almada**[1], **Kerry J. Ressler**[2], **Carsten T. Wotjak**[1], **Valery Grinevich**[4], **Alon Chen**[1], **Mathias V. Schmidt**[1], **Wolfgang Wurst**[5,6,7], **Damian Refojo**[1,8], **Jan M. Deussing**[1,*]

[1]Department of Stress Neurobiology and Neurogenetics, Max Planck Institute of Psychiatry, Munich, Germany.

[2]Department of Psychiatry, Harvard Medical School and McLean Hospital, Belmont, MA, USA.

[3]Laboratory of Neuropsychopharmacology, Paulista State University, Araraquara, Brazil.

[4]Schaller Research Group on Neuropeptides, German Cancer Research Center, Central Institute of Mental Health, University of Heidelberg, Heidelberg, Germany.

[5]Institute of Developmental Genetics, Helmholtz Zentrum München, Munich, Germany.

[6]Technische Universität München, Chair of Developmental Genetics, Munich, Germany.

[7]German Center for Neurodegenerative Diseases (DZNE), Site Munich, Munich, Germany.

[8]Instituto de Investigacion en Biomedicina de Buenos Aires (IBioBA)-CONICET-Partner Institute of the Max Planck Society, Buenos Aires, Argentina.

[9]These authors contributed equally: Nina Dedic, Claudia Kühne.

Abstract

The interplay between corticotropin-releasing hormone (CRH) and the dopaminergic system has predominantly been studied in addiction and reward, while CRH-dopamine interactions in anxiety are scarcely understood. We describe a new population of CRH-expressing, GABAergic, long-range-projecting neurons in the extended amygdala that innervate the ventral tegmental area and

*Correspondence and requests for materials should be addressed to J.M.D. deussing@psych.mpg.de.

Author contributions

N.D. and C.K. designed and performed experiments and analyzed data. N.D. and J.M.D. wrote the manuscript. M.J., J.H., K.S.G., M.L.P., S.C., A.K., A.M.V, M.W.M., B.S. and R.C.A. assisted with behavioral experiments and tracing and imaging experiments. E.A., J.D. and A.J.G. conducted microdialysis, electrophysiology and optogenetic experiments, respectively. K.J.R., C.T.W., V.G., A.C., M.V.S., W.W. and D.R. contributed to methodology and resources. J.M.D. designed experiments, analyzed data and supervised the project.

Competing interests

The authors declare no competing financial interests.

Supplementary information is available for this paper at https://doi.org/10.1038/s41593-018-0151-z.

alter anxiety following chronic CRH depletion. These neurons are part of a distinct CRH circuit that acts anxiolytically by positively modulating dopamine release.

CRH and its type 1 high affinity receptor (CRHR1) are widely distributed throughout the brain[1–3] and modulate neuroendocrine and higher order behavioral responses to stress[3]. Although it is widely accepted that CRH-CRHR1 signaling induces aversive stress-like behavioral responses, we and others have recently shown that CRH and CRHR1 can also act in an anxiolytic and appetitive manner via interaction with the dopaminergic system[1,4]. The ventral tegmental area (VTA) and substantia nigra pars compacta (SNc) express high levels of CRHR1[1,3], and conditional deletion of *Crhr1* in dopaminergic neurons increases anxiety and reduces dopamine release in the prefrontal cortex[1], suggesting the presence of an anxiolytic CRH-CRHR1 circuit. However, the source of CRH in the VTA remains controversial[5–8]. Here we aimed to determine the origin and identity of VTA-targeting CRH neurons and unravel their specific role in modulating positive emotional responses.

CRH is heavily expressed in structures of the extended amygdala, including the anterior bed nucleus of the stria terminalis (aBNST) and the lateral part of the central amygdala (CeA)[2,3,9,10], two brain regions critically involved in the regulation of fear and anxiety[6,9–12]. To determine whether these CRH neurons project to the VTA, we injected AAVs expressing a Cre-dependent synapto-physin-GFP (Syp-GFP) fusion protein into different brain regions of *Crh-ires-Cre* mice. Presynaptic Syp-GFP puncta in the VTA and SNc were most dense following tracer injection into the aBNST and CeA (Fig. 1a,b, Supplementary Figs. 1 and 2 and Supplementary Table 1), demonstrating the presence of VTA-innervating CRH neurons in the extended amygdala, which has also been suggested by others[13,14].

Double in situ hybridizations revealed an overwhelming majority of GABAergic CRH neurons in the aBNST and CeA and confirmed[9,10] the distinct identity of CeA CRH neurons that were *Gad65/67*-positive (expressing glutamate decarboxylases *Gad1* and/or *Gad2*) but largely protein kinase Cδ- and somatostatin-negative (not expressing *Prkcd* or *Sst*) (Fig. 1c and Supplementary Figs. 3 and 4a–c). By contrast, most *Crh* neurons in the piriform cortex coexpressed the glutamatergic marker *Vglut1* while 29.9 ± 2.1% in the paraventricular nucleus of the hypothalamus colocalized with *Vglut2*, highlighting the diversity of CRH neurons in different brain regions. Overall, these results suggest that VTA-targeting CRH neurons of the aBNST and CeA represent GABAergic long-range projection neurons.

Intriguingly, morphological assessment in *Crh-ires-Cre;Ai32(ChR2)* mice revealed the presence of thin and mushroom-like dendritic spines in a subgroup of CRH neurons in the aBNST and CeA (Fig. 1d). Dendritic spines are conventionally believed to be largely absent from inhibitory neurons. Notably, we primarily detected aspiny GABAergic CRH neurons in the hippocampus and cortex (Supplementary Fig. 4d–f), which have previously been ascribed to classical, locally projecting interneurons including basket, chandelier and double bouquet cells[15,16].

Notably, approximately one-third of *Crh* neurons in the aBNST and CeA coexpressed calcium/calmodulin-dependent protein kinase 2α (*Camk2a*) (Fig. 2a and Supplementary Fig. 3), one of the most abundant postsynaptic density proteins, which is crucial for several

aspects of synaptic plasticity[17] and is predominantly expressed in excitatory pyramidal neurons of the forebrain. Accordingly, *Crh*-expressing glutamatergic neurons in the piriform cortex also coexpressed *Camk2a* (Supplementary Fig. 3). However, CAMK2A signaling is also important in medium spiny neurons of the striatum[17,18], the most prominent population of spiny, GABAergic, long-range projecting neurons in the brain. In addition, VTA-projecting GABAergic CAMK2A neurons have been identified in the BNST and were shown to produce rewarding and anxiolytic phenotypes upon optogenetic activation[11]. We validated the presence of triple-positive GABAergic CAMK2A CRH neurons in the aBNST and CeA by combining a recombinase-based intersectional mouse genetic strategy with CRH immunohistochemistry (Fig. 2b,c and Supplementary Fig. 5).

Next we labeled CAMK2A-expressing CRH neurons by injecting AAV-Camk2a::DIO-EYFP into the aBNST and CeA of *Crh-ires-Cre* mice. Dendrites of CAMK2A CRH neurons were sparsely to moderately decorated with thin and mushroom-like spines, which received presynaptic input as evidenced by synaptophysin labeling (Fig. 2d,e). Moreover, we observed dense EYFP labeling in fibers within the VTA and SNc following AAV-Camk2a::DIO-EYFP injections into the CeA or aBNST (Fig. 2f and Supplementary Fig. 6). Analysis after CLARITY tissue clearing of *Crh-ires-Cre* mouse brains injected with AAV-Camk2a::DIO-EYFP additionally demonstrated that the VTA and SNc represent primary projection targets of aBNST CAMK2A CRH neurons (Fig. 2g and Supplementary Video 1). Collectively, these results suggest that VTA-projecting CRH neurons in the aBNST and CeA represent a previously undefined class of largely spiny, CAMK2A-expressing, GABAergic long-range projection neurons. Although the majority of CAMK2A CRH neurons had spines, we were not able to accurately quantify the percentage of total spiny vs. aspiny neurons due to the dense local projections and intermingled dendrites of CeA aBNST CRH neurons.

To target the identified CAMK2A-CRH circuit, we generated conditional *Crh* knockout mice (Crh^{flox}), crossed them with *Camk2a-CreER*^{T2} mice and induced the knockout in adulthood via tamoxifen-containing food (Fig. 3a and Supplementary Fig. 7). As expected, loss of *Crh* expression in the resulting $Crh^{CKO\text{-}Camk2a}$ mice was primarily observed in the aBNST and CeA, but also in *Crh*-expressing glutamatergic neurons of the piriform cortex (Fig. 3b,c and Supplementary Fig. 8a,b). On the basis of our finding that deletion of *Crhr1* in dopaminergic neurons increases anxiety[1], we assessed whether lack of *Crh* from VTA-projecting CAMK2A CRH neurons would result in similar effects. Compared to littermate controls, $Crh^{CKO\text{-}Camk2a}$ mice displayed increased anxiety in the open field, dark-light box, elevated plus-maze (EPM) and marble burying test, which was independent of altered corticosterone release (Fig. 3d–f and Supplementary Fig. 8c,d). The anxious phenotype did not result from *Crh* absence in *Camk2a*-expressing glutamatergic neurons, since deletion of *Crh* specifically in glutamatergic neurons (Crh^{fox} × *Nex-Cre*, expressing Cre under the *Neurod6* promoter) did not induce behavioral alterations (Supplementary Fig. 9). In view of CRH's importance in conditioned fear[3] and recent findings demonstrating that CeA CRH neurons mediate conditioned flight[12] and are required for discriminative fear[9], we also assessed auditory and contextual fear conditioning. $Crh^{CKO\text{-}Camk2a}$ mice displayed increased freezing upon reexposure to the tone (Fig. 3g), which was most prominent after termination of the conditioned stimulus. Notably, contextual fear memory was not altered (Supplementary Fig.

8e). Additional experiments revealed higher levels of sensitized fear to an unsignaled tone in *Crh*$^{CKO\text{-}Camk2a}$ mice, suggesting overall impairments in the readjustment of fear levels rather than alterations in fear memory formation (Supplementary Fig. 8f–h).

CRH is known to activate dopamine neuron firing and induce dopamine release[4,7,19], while deletion of *Crhr1* in dopaminergic neurons reduces dopamine release in the prefrontal cortex[1], a structure critically involved in the modulation of anxiety and a major target of the mesocortical dopamine circuit. Applying in vivo microdialysis, we observed a significant reduction in absolute dopamine release in the prefrontal cortex of *Crh*$^{CKO\text{-}Camk2a}$ mice, both under baseline conditions and following footshock stress (Fig. 3h). However, the magnitude of the response to the acute footshock was similar (Supplementary Fig. 8j), indicating generally lower dopamine levels in *Crh*$^{CKO\text{-}Camk2a}$ mice rather than alterations in stress-induced synaptic dopamine release. We detected no differences in dopamine levels in the nucleus accumbens (Supplementary Fig. 8l).

Next we investigated potential compensatory changes in CRHR1, CRHR2 and urocortin (UCN) expression in *Crh*$^{CKO\text{-}Camk2a}$ mice. Quantitative PCR analysis revealed a significant upregulation of *Crhr1* alone in the VTA of *Crh*$^{CKO\text{-}Camk2a}$ mice, further supporting the involvement of CAMK2A-positive CRH neurons in CRHR1-VTA signaling (Supplementary Fig. 8m). To determine whether behavioral alterations in *Crh*$^{CKO\text{-}Camk2a}$ mice are caused by a lack of CRH from CAMK2A-positive aBNST CeA neurons or by compensatory upregulation of *Crhr1* in the VTA, we explored the direct impact of enhanced CRH-CRHR1 signaling in the VTA on anxiety and fear conditioning. For this, we first generated a *Crhr1-ires-Cre* driver in which Cre-expression faithfully reproduces the endogenous *Crhr1* expression pattern without compromising either its expression or corticosterone release (Supplementary Figs. 10 and 11). Using *Crhr1-ires-Cre* mice, we expressed a constitutively active (CA) version of CRHR1 fused to EGFP (AAV-DIO-CA(CRHR1)-EGFP)[20] specifically in CRHR1-expressing VTA neurons (Fig. 3i and Supplementary Fig. 12a). CA(CRHR1) mice exhibited decreased anxiety-related behavior in the dark-light box, EPM and marble burying test (Fig. 3j–l), without displaying changes in fear conditioning (Fig. 3j–m and Supplementary Fig. 12). This suggests that enhanced CRHR1 signaling in the VTA promotes decreased anxiety without altering fear memory expression. Similarly, intra-VTA microinjections of CRH (40 ng/side) in wild-type mice partially decreased anxiety without altering fear levels. However, a lower dose of CRH did not induce behavioral changes, while a higher dose significantly impaired locomotion (Supplementary Fig. 13), indicating dose-specific effects on general behavior following exposure to exogenous (potentially nonphysiological) CRH levels. The fact that neither VTA-specific expression of CA(CRHR1) nor microinjections of CRH affected cued freezing lets us speculate that increased fear memory expression in *Crh*$^{CKO\text{-}Camk2a}$ mice is a consequence of CRH absence from locally projecting CeA neurons[9] and/or other long-range projection neurons.

Notably, photoexcitation of VTA-innervating, ChR2-expressing CRH terminals did not alter anxiety and fear memory expression (Supplementary Fig. 14). However, acute optogenetically mediated activation or inhibition of CRH fibers, which is likely to influence the co-release of GABA and presumably other neurotransmitters, cannot be directly compared to chronic manipulation of CRH alone. Consequently, our results imply that

prolonged dysregulation of CRH-release from VTA-targeting extended amygdala neurons and/or chronic changes in CRHR1 signaling in the VTA are required to induce alterations in anxiety-related behavior.

Previous work has repeatedly demonstrated an aversive or anxiogenic role for CRH-CRHR1 signaling in the VTA of drug-experienced animals[5,8]. Thus, it is likely that CRH release in the VTA can exert opposing effects on anxiety under baseline and drug- or stress-induced conditions[4].

Collectively our results suggest that a subpopulation of CRH-and CAMK2A-expressing, GABAergic projection neurons of the extended amygdala target CRHR1 on dopaminergic VTA neurons to positively modulate emotional behavior by regulating dopaminergic neurotransmission (Supplementary Fig. 15). This reveals a previously unidentified anxiolytic CRH circuit and further establishes the presence of opposing CRH networks in the regulation of stress-related emotional behavior.

Methods

Methods, including statements of data availability and any associated accession codes and references, are available at https://doi.org/10.1038/s41593-018-0151-z.

Methods

Animals.

All animal experiments and protocols were legally approved by the Ethics Committee for the Care and Use of Laboratory Animals of the government of Upper Bavaria, Germany. All mice were group housed (maximum four mice per cage) under standard laboratory conditions (22 ± 1 °C, 55 ± 5% humidity) with a 12:12 h light:dark schedule with food and water provided ad libitum. All experiments were performed in 10- to 14-week-old male mice other than (i) corticosterone measurements in *Crhr1-ires-Cre* mice, which were performed in female mice (Supplementary Fig. 11d) and (ii) VTA-expression of CA(CRHR1), which was performed in 6- to 9-week-old male mice (Fig. 3i–j and Supplementary Fig. 12). Behavioral testing and microdialysis were conducted between 8:30 a.m. and 12:30 p.m. during the light cycle. Mice were single housed 1 week before behavioral testing and hormone assessment. For all experiments with inducible Cre recombinase lines, tamoxifen was given in food pellets (LAS CRdiet CreActive TAM400, LASvendi) during postnatal weeks 10–12, and analyses were performed 1–2 weeks later. Morphological assessment of CRH neurons was conducted in *Crh-ires-Cre* mice[21] bred to *Ai9* (*R26*$^{CAG:hxP\text{-}STOP\text{-}oxP\text{-}idTcmao}$, stock no: 007905) or *Ai32* (*R26*$^{CAG::loxP\text{-}STOP\text{-}loxP\text{-}ChR2\text{-}EYFP}$, stock no: 012569)[22] mice, which were purchased from the Jackson Laboratory. Conditional *Crh* knockout mice (see “Generation of conditional knockout mice” below) lacking *Crh* ubiquitously, in glutamatergic and in CAMK2A-expressing neurons were generated by crossing *Crh*^{flox} mice with Cre Deleter (purchased from TaconicArtemis, Cologne, Germany), *Nex-Cre*[23] and *Camk2a-CreER*^{T2} mice[24], respectively. Intersectional fate-mapping was performed in RC::FrePe mice[25,26], bred to Dlx5/6-Flp[27] (purchased from Jackson Laboratory, stock no: 010815) and *Camk2a-CreER*^{T2} mice.

Generation of conditional *Crh* knockout mice.

Mice with a floxed *Crh* allele (*Crh*^{flox}) were generated based on the previously described strategy used to generate *Crhr1*-reporter mice and conditional *Crhr1* knockout mice[28]. The targeting vector was constructed from a universal shuttle vector with an inverted diphtheria toxin A (DTA) expression cassette for negative selection. The shuttle vector comprises the following components, which were flanked by *attP* sites, thereby enabling cassette exchange in embryonic stem (ES) cells subsequent to homologous recombination (from 5′ to 3′): 5′ homology arm, including *Crh* exon 1 and the 5′ part of intron 1, upstream *loxP* site, first *frt* site, adenovirus splice acceptor (SA), *tau-lacZ* (*tZ*) reporter gene equipped at its C terminus with a *flag* tag, second *frt* site and a reverse-oriented *EM7*-neo positive selection cassette, including a bovine growth hormone polyadenylation signal. Finally, downstream of the second *attP* site there was a reverse-oriented *Pgk1* promoter, a third *frt* site, the 3′ part of intron 1, as well as exon 2 with the downstream *loxP* site inserted in the 3′ UTR, and the 3′ homology arm (see also Supplementary Fig. 7). The linearized (*ScaI*) targeting vector was electroporated into TBV2 ES cells (129S2). Mutant ES cells were identified by Southern blot analysis of genomic ES cell DNA digested with EcoRI (5′ probe) and BamHI (3′ probe), respectively. Mutant ES cells were used to generate chimeric mice by blastocyst injection. Male chimeras were bred to wild-type C57BL/6 J mice and germline transmission of the modified *Crh* reporter allele (*Crh*^{tz}) was confirmed by PCR in F1 offspring. Breeding the *Crh*^{tz} reporter mice with transgenic Flpe Deleter mice[29] led to deletion of the *tZ-neo* cassette and resulted in a conditional *Crh* allele (*Crh*^{flox}) leaving exon 2 flanked by *loxP* sites. Subsequent breeding to Cre driver lines resulted in conditional deletion of the *loxP* flanked *exon 2* (*Crh*^{CKO}). Mice were of a mixed 129S2/Sv × C57BL/6 J genetic background.

Generation of *Crhrl-ires-Cre* mice.

Mice expressing Cre recombinase under the control of the *Crhr1* promoter were generated by using a recombinase-mediated cassette exchange (RMCE) strategy. ES cell clones carrying a respective docking site in intron 2 of the *Crhr1* gene were generated previously[28]. In contrast to the *Crhr1*^{Z} allele, the ES clone used for RMCE did not contain a *loxP* site 5′ of exon 2 (*Crhr1*$^{tZ\text{-}\Delta loxP}$; see also Supplementary Fig. 10) The *attB* site-flanked *Crhr1-Cre* recombinase expression unit encompassed, from 5′ to 3′, *Crhr1* intron 2 (3′ of the original BglII insertion site) to exon 3 fused to the *Crhr1* cDNA covering exons 4–13, an *ires-Cre* cassette with a bGH-pA, and a *frt* site followed by a *Pgk1* polyadenylation sequence and hygromycin resistance cassette, both in inverse orientation. φC31 integrase-mediated cassette exchange resulted in insertion of the *Crhr1-Cre* expression unit into the right *attP* site as verified by PCR and sequencing (*Crhr1*$^{tZ\text{-}iCre}$). Mutant ES cells were used to generate chimeric mice that transmitted the modified *Crhr1* allele through the germline. The *tau-lacZ* reporter and hygromycin selection cassette were removed by breeding to *FLPeR* mice[30]. Selective removal of both cassettes was demonstrated by PCR on genomic DNA from offspring using primers A (Flipase-1-fwd) 5′-GAC-CTG-CAG-GAA-CCA-ACT-GT-3′, B (Primer-2-Cre-rev) 5′-CAC-CCA-TGG-TTA-GTC-CCA-GT-3′, C (P-Cre-downs-fwd2) 5′-AAT-AAT-AAC-CGG-GCA-GGG-GG-3′, D (Flipper-rev-1) 5′-CGA-CTA-GAG-CTT-GCG-GAA-CCC-3′, E (P-PGK-fwd2) 5′-CCT-ACC-GGT-GGA-TGT-GGA-AT-3′, F (Cre-fwd) 5′-GAT-CGC-TGC-CAG-GAT-ATA-CG-3′, G (Cre-rev) 5′-AAT-CGC-CAT-CTT-CCA-GCA-G-3′, Thy1-F1 5′-TCT-GAG-TGG-CAA-AGG-ACC-TTA-GG-3′ and Thy1-R1

5′-CCA-CTG-GTG-AGG-TTG-AGG-3′ (see also Supplementary Fig. 10). Mice were kept on a mixed 129S2/Sv × C57BL/6 J genetic background.

Production of adeno-associated viruses (AAVs).

The synaptophysin-GFP coding sequence (original construct[31]) was subcloned into a double-floxed inverted open-reading frame (DIO) vector under the control of the *Ef1a* promoter (Ef1a::DIO-eYFP, Addgene, #27056). The Camk2a::DIO-EYFP construct was created by replacing the *Ef1a* promoter in the Ef1a::DIO-EYFP construct with a 1.5-kb *Camk2a* promoter fragment. Packaging and purification of recombinant (r) AAVs (serotype 1/2) was conducted as previously described[32]. rAAV titers were ~10^{10} genomic copies per microliter. The Ef1a::DIO-(CA) CRHR1-EGFP vector was kindly provided by Benjamin Arenkiel[20,33] (Baylor College of Medicine, Houston, TX) and packaged into $AAV_{1/2}$. $AAV_{1/2}$-Ef1a::DIO-mCherry was used as a control (vector purchased from Addgene; plasmid 50462, donated by Bryan Roth).

Stereotactic surgeries.

For all experiments using stereotactic surgeries (viral injections for tracing experiments, optic fiber or guide cannula placements for CRH microinfusions and in vivo microdialysis), mice were anesthetized with isoflurane (Floren, Abbott), 2% v/v in O_2 and placed in a stereotaxic apparatus (TSE Systems Inc., Bad Homburg, Germany) with adapted components to allow mouse inhalation anesthesia. Post-surgery recovery included Metacam supplementation, 0.25 mg per 100 ml with drinking water, for 3 d after surgery, with daily inspection of food intake. At the end of the experiments, mice were killed with an overdose of isoflurane (Floren, Abbott) and transcardially perfused with PBS followed by 4% PFA, and brains removed for subsequent analysis. For viral injections, CRH microinfusions and optogenetic experiments, brains were sectioned (40 μm) using a vibratome (Microm HM 650 V, Thermo-Fisher Scientific) and accurate placements of microinjection cannulas and optic fibers verified. For microdialysis experiments, brains were sectioned using a cryostat (Leica CM 3000) and accurate probe placements verified.

Viral injections and tracing analyses.

Crh-ires-Cre mice were unilaterally injected with either AAV-Ef1a::DIO-Syp-GFP or AAV-Camk2a::DIO-EYFP into the dorsal and ventral part of the aBNST (350 nl dorsal + 350 nl ventral), CeA (300 nl), PVN (250 nl), piriform cortex (250 nl) and prefrontal cortex (400 nl) using a 33-gauge microinjection needle with a 10-μl syringe (Hamilton) coupled to an automated microinjection pump (World Precision Instruments Inc.) at 100 nl/min. Coordinates in millimeters from bregma were as follows: aBNST (A/P + 0.15, M/L ± 0.8, D/V −4.25 and −4.75), CeA (A/P −1.0, M/L ± 2.6, D/V −4.5), PVN (A/P −0.80, M/L ± 0.25, D/V −4.75). At the end of the infusion, needles were kept at the site for 10 min and then slowly withdrawn. Viral expression was assessed 4 weeks after surgery.

Fluorogold (Fluorochrome, LLC) was dissolved as 1% w/v in 0.9% saline and 0.3 μl were injected unilaterally in the VTA. Retrobeads were obtained from Lumafluor Inc and injected undiluted in a volume of 100 nl. VTA coordinates in millimeters from bregma: A/P −3.0, M/L ± 0.6 and D/V 4.5. Mice were killed and brains assessed 4 d after surgery.

Microdialysis and dopamine measurements.

Microdialysis was performed as described previously[34]. Guide cannulas were implanted unilaterally into the right medial prefrontal cortex (coordinates in millimeters from bregma: A/P 2.20, M/L 0.35 and D/V 1.50). One day before the experiment, CMA 11 metal-free microdialysis probes with a cuprophane membrane of 2 mm length and o.d. of 0.2 mm (CMA Microdialysis) were inserted and connected to the perfusion lines consisting of FEP tubing and a low-volume liquid swivel TCS2–23 (EiCOM). From the moment of insertion, probes were continuously perfused with sterile artificial cerebrospinal fluid (in mM: NaCl, 145; KCl, 2.7; $CaCl_2$, 1.2; $MgCl_2$, 1.0; Na_2HPO_4, 2.0; pH 7.4) at a flow rate of 0.3 μl/min.

On the experimental day, following a 1 h equilibration period, 20-min microdialysis fractions were constantly collected in cooled 300-pl microtubes (Milian AG) containing 2 μl of 0.1 M perchloric acid at a perfusion rate of 1.1 μl/min. The dead volume of the outlet line was compensated by a delay in fraction harvesting (10 min). Six consecutive baseline samples were collected. Thereafter, mice were placed into a custom-made shock chamber for a total of 5 min. After 180 s of habituation, animals underwent two electric foot shocks (1.5 mA, 2 s long) with a 60-s interval in between. Animals remained in the shock chamber for another 60 s before being returned to their microdialysis home cages.

Dopamine content in the microdialysates was determined by reversed-phase high-performance liquid chromatography (HPLC) with electrochemical detection (UltiMate3000 HPLC system, Coulochem III, Thermo-Fisher Scientific). All reagents used for the phosphate-citrate mobile phase (methanol 10%, pH 5.6) were of analytical grade (Carl Roth GmbH or Merck KGaA). Monoamines were separated on an analytical column (C18, 150 × 3 mm, 3 μm; YMC Triart, YMC Europe GmbH) at a flow rate of 0.4 ml/min. The potentials of the working electrodes were set to 75 mV and 250 mV, and the guard cell potential was set at 350 mV Dopamine concentrations were calculated by external standard curve calibration using the peak area for quantification. The detection limit for dopamine was 0.032 nM.

Intra-VTA CRH infusions.

Stainless steel cannulas (8 mm) were inserted bilaterally above the left and right VTA (A/P −3.2 mm, M/L ± 0.5 mm, D/V −3.6 mm). A small screw was drilled into the skull to affix the protective helmet. The screw and the cannulas were fixed to the skull by the application of dental cement (Paladur, Heraeus Kulzer). Following surgery, animals were allowed to recover for 1 week. Mice were infused with 0.4, 40 or 400 ng CRH (Bachem #H-2435.001, 1 mg) per side dissolved in aCSF. 500 nl/side were delivered at an infusion rate of 0.1 μl/min using injectors that protruded 1 mm beyond the cannulas. Vehicle animals received aCSF only. Mice were tested 30 min after vehicle or CRH injection. Separate cohorts (vehicle and CRH treated) were used for each CRH dose (0.4, 40 and 400 ng/side). Each behavioral test was performed on a separate day for each CRH dose tested. The tests were conducted in the following order: open field, dark-light, EPM and fear conditioning.

Optogenetic stimulation.

Optogenetic activation of CRH-positive terminals within the VTA was performed in *Crh-ires-Cre* mice bred to ChR2-EYFP-expressing Ai32 mice. *Crh-ires-Cre;Ai9(tdTomato)* mice were used as respective controls. Optic fibers (200 μm, NA 0.39, Thorlabs CFML12L20 cut to 7 mm length) were implanted bilaterally above the VTA using the following coordinates, in millimeters: AP −3.2, ML ± 0.55, -DV 3.8, with an angle of ± 10°, and secured with dental acrylic (Paladur, Heraeus Kulzer). After the stereotaxic surgery, the animals were left for 2 weeks to recover. The laser (Omikron LightHUB-4, 460 nm) output power was adjusted to read 12 mW measured at the fiber tip. The laser was pulsed at 20 Hz with 15 ms pulse width, using an external pulse stimulator (Master-8, A.M.P.I.). Bilateral stimulation of freely moving animals was achieved using a fiber-optic rotary joint (FRJ_1 × 2i_FC-2FC, Doric).

For the dark-light test, laser stimulation was initiated 5–10 s before the animals were placed into the dark compartment and lasted for 420 s.

The EPM was divided into three alternating 5-min epochs: laser stimulation off, stimulation on and stimulation off (OFF-ON-OFF epochs).

Auditory cued fear conditioning was performed as described in the “Fear conditioning” section below. Optogenetic stimulation took place only during the second minute of tone presentation (60 s). Freezing was scored with the tracking software ANY-maze (Stoelting Co.).

VTA-specific expression of a constitutively active CRHR1.

Crhr1-ires-Cre mice were bilaterally injected with AAV-Ef1a::DIO-(CA)CRHR1-EGFP or the control virus AAV-Ef1a::DIO-mCherry in the VTA (0.3 μl/side) at a rate of 0.10 pl/min using a Neuros series Hamilton syringe (Reno, NV) connected to microinjection pump (World Precision Instruments). Coordinates in millimeters for VTA injections were A/P −3.0, M/L ± 0.6, D/V −4.6. Behavioral experiments (open field, dark-light, EPM, marble burying and fear conditioning, as described below) were started at least 3 weeks after surgery.

Immunofluorescence staining.

Immunofluorescence staining was performed as previously described[1]. Briefly, brain slices were permeabilized with PBS-Triton X-100 0.1%, blocked at room temperature for 1 h in 5% BSA in PBS-Triton X-100 0.1%, and incubated overnight (or longer) at 4 °C with the primary antibody. On the next day, slices were washed and incubated with the secondary antibody for 2 h at room temperature. After a final wash, brain slices were stained with DAPI and mounted with anti-fading fluorescence VectaShield medium (Vector Laboratories). Primary antibodies: anti-tyrosine hydroxylase (#P40101, 1:2,000, PelFreez Biologicals), anti-synaptophysin (#ab14692, 1:2,000, Abcam), anti-CRH, 1:20,000, 1 week incubation; obtained from Paul E. Sawchenko, Salk Institute, CA). Specificity of the anti-CRH antibody has previously been validated[35,36]. Secondary antibodies (1:2,000): Alexa

Fluor 594 goat anti-rabbit IgG (#A11037, Invitrogen Life Technologies), Alexa Fluor 647 goat anti-rabbit IgG (#A21244, Invitrogen Life Technologies).

Image acquisition.

Images were captured with either a Zeiss Axioplan2 fluorescence microscope and Axio Vision 4.5 software or an Olympus IX81 inverted laser scanning confocal microscope and Fluoview 1000 software. For confocal imaging, a *z*-stack of pictures of areas of interest was obtained with 0.4–1.2 μm step size and 800 × 800 to 1,024 × 1,024 pixel picture size. Images were analyzed with ImageJ (https://imagej.nih.gov/ij/) and Adobe Photoshop CS2.

In situ hybridization (ISH) and double ISH.

Brains were sectioned coronally at 20 μm using a cryostat (Microm, Walldorf, Germany). The sections were thaw-mounted onto SuperFrost slides, dried, and kept at −80 °C. Single and double ISH was performed as previously described[1,37,38]. The following riboprobes were used: *Gad67* (*Gad1*): bp 984–1940 of NM_008077; *Gad65* (*Gad2*): bp 753–1600 of NM_008078; *Vglut1* (*Slc17a7*): bp 1934–2550 of NM_182993; *Vglut2* (*Slc17a6*): bp 2427–3006 of NM_080853.3; *Crh* (3′ UTR): bp 2108–2370 bp of AY128673; *Camk2a*: bp 2034–2903 of NM_177407.4; *Tomato*: bp 740–1428 of AY678269. Quantifications of double and single ISHs were performed blindly using the freely available NIH ImageJ software (https://imagej.nih.gov/ij/).

CLARITY.

Mice were perfused with 20 ml of 0.1 M PBS at 4 °C, followed by 20 ml of a hydrogel solution containing 4% acrylamide, 0.05% bisacrylamide, 0.25% VA-044 Initiator, 4% PFA and 0.1 M PBS at 4 °C. Brains were extracted and incubated in hydrogel solution at 4 °C for 3 more days, then incubated at 37 °C for 3 h until the hydrogel solution had polymerized. Subsequently, the tissue was washed in a clearing solution containing 200 mM boric acid and 4% sodium dodecyl sulfate with pH 8.5 for 2 d at 37 °C. After 1 week of incubation in clearing solution at 37 °C, electrophoretic tissue clearing was performed for 5 d in the clearing solution at 37 °C and 15 V. Following another week of incubation in the clearing solution at 37 °C, the sample was washed twice for 24 h with PBST (0.1% Triton X in 0.1 M PBS). The cleared brain was incubated in FocusClear (CelExplorer Labs Co., Hsinchu, Taiwan) for 2 h before imaging with a LaVision Light Sheet microscope (LaVision BioTec, Duisburg, Germany). A movie compiled from individual *z*-stack images was created with ImageJ (https://imagej.nih.gov/ij/).

Open field, dark-light box and elevated plus-maze (EPM) tests.

The open field test was used to assess general locomotion and anxiety-related behavior and was conducted in an evenly illuminated (<15 lx) square apparatus (50 × 50 × 60 cm). The test duration was 15 min. The dark-light box and EPM were employed to assess anxiety-related behavior. The dark-light box test was performed for 5 min in apparatus consisting of a secure black compartment (<5 lx) and an aversive, brightly illuminated white compartment (700 lx). The EPM consisted of a plusshaped platform with four intersecting arms, elevated 37 cm above the floor. Two opposing open (30 × 5 cm) and closed (30 × 5 × 15 cm) arms

were connected by a central zone (5 × 5 cm). Animals were placed in the center of the apparatus facing the closed arm and were allowed to freely explore the maze for 5 min. Open arm time was calculated as a percentage of time in seconds: open arm time (%) = open arm time/(open arm time + closed arm time). All experiments were analyzed using the automated video-tracking system ANYmaze (Stoelting, Wood Dale, IL).

Marble burying test.

Mice were placed into a housing cage (Green Line IVC Sealsafe PLUS Mouse, Techniplast) filled with corn cob bedding (5 cm high) and containing 10 black marbles, evenly distributed over the surface of the corn cob layer. After the cages had been covered with flipped cage lids, animals were allowed to roam the cages freely for 1 h. At the end of the test period the number of buried marbles was assessed by an observer blind to the genotype.

Fear conditioning.

Contextual and cued fear conditioning was performed in conditioning chambers (ENV-307A, MED Associates Inc.) as previously described[39]. Foot shock (FS) delivery and context-dependent fear memory were assessed in a cube-shaped chamber with metal grid floors, which was thoroughly cleaned and sprayed with 70% ethanol before the animals were introduced (shock context). A neutral context consisting of a Plexiglas cylinder with bedding was used to investigate cued (tone-dependent) fear memory; it was cleaned and sprayed with 1% acetic acid (novel context). For foot shock application (day 0), mice were placed into the conditioning chamber for 3 min. After 180 s, a sine wave tone (80 dB, 9 kHz) was presented for 20 s, which coterminated with a 2 s scrambled electric foot shock of 1.5 mA. The mice remained in the shock chamber for another 60 s. To measure the freezing responses to the tone, mice were placed into the novel environment (cylinder) on the following day (day 1). Three minutes later, a 3-min tone was presented (80 dB, 9 kHz). The animals were returned to their home cages 60 s after the end of tone presentation. Contextual fear was tested by reexposing the animals to the shock context for 3 min on day 2. As a measure of fear memory, freezing behavior was recorded and analyzed by an observer blind to genotype. Freezing was scored if the animals adopted an immobile posture (except for breathing-related movement) with all four paws on the ground and the head in a horizontal position. Data were analyzed in 20-s, 60-s or 180-s bins and normalized to the observation interval as indicated in the Results section.

Pain perception and shock-related fear sensitization.

Individual pain thresholds were determined essentially as described before[40,41]. In brief, on day 0 mice were individually placed into the shock chamber. After 3 min baseline, current intensity of the foot shock was constantly increased at 5 μA/s until the mice showed first signs of discomfort (backwards moving; PT1) and pain (jumping and vocalization; PT2) and the respective current intensities were noted. Once mice showed those signs of pain, the current was immediately switched off. Behavioral performance was judged by trained observers blinded to genotype.

To further investigate shock-related fear sensitization, all mice received an unsignaled electric foot shock of 1.5 mA (2 s) within 15 s after determination of PT2 on day 0 and

returned to their home cages 60 s later. The next day (day 1), animals were placed into the novel context. After a baseline period of 3 min, a sine-wave tone (9 kHz, 80 dB, 3 min) was presented for the first time, and mice were placed back to their home cage 60 s after tone offset. This procedure allows measurement of nonassociative memory components of the conditioning procedure[39,42–45]. On day 2, mice were reexposed to the shock chamber for 3 min. Generalization of contextual fear was assessed by comparing the freezing responses shown (i) before shock presentation at day 0, (ii) during exposure to the novel context before the subsequent tone presentation (day 1) and (iii) during reexposure to the shock context (day 2). Freezing behavior was recorded and analyzed by an observer blind to the genotype as described above.

Corticosterone measurements.

Plasma corticosterone concentrations were measured as previously described[1] using a commercially available RIA kit (MP Biomedicals, Eschwege, Germany) according to the manufacture's manual.

qPCR analysis.

Tissue punches for respective brain regions were collected from coronal cryosections with a punching tool (FST, 1 mm diameter) directly into ice-cold Trizol reagent (Invitrogen) and stored at −80 °C until RNA isolation. Total RNA was isolated following the Trizol protocol and the aqueous phase was purified using Qiagen RNAeasy columns and buffers. RNA templates were transcribed into cDNA with the Superscript III kit (Invitrogen) and random hexamer primers. cDNA was amplified on a Roche LightCycler 96 System with Fast SYBR Green PCR Master Mix (Roche). Specific primers and *Hprt* housekeeping primers were as follows: *Crhr1* (fwd. 5′-GGG-CCA-TTG-GGA-AAC-TTT-A-3′; rev. 5′ - AT C - AGC - AG G - AC C - AGG - AT C - A- 3′), *Ucn1* (fwd. 5′-TCT-TGC-TGT-TAG-CGG-AGC-G-3′; rev. 5'-TCG-AAT-ATG-ATG-CGG-TTC-TGC-3′), *Hprt* (fwd. 5′-GTT-CTT-TGC-TGA-CCT-GCT-GGA-3′; rev. 5′-TCC-CCC-GTT-GAC-TGA-TCA-TT-3′).

Electrophysiological recordings.

Brain slices were prepared as described before[46] in carbogenated choline chloride–based solution. Slices 300 μm thick at the level of the CeA were hemisected along the midline and incubated for 30 min in carbogenated artificial cerebrospinal fluid (aCSF) at 34 °C. After 60 min recovery at room temperature, a hemislice was transferred and submerged in the recording chamber, in which it was continuously perfused (4–5 ml/min) with aCSF at room temperature. Patch-clamp recordings were carried out at 25 °C as previously described[46]. The patch-clamp electrodes (open-tip resistance 5–7 MΩ) were filled with a solution consisting of (in mM) 130 potassium gluconate, 5 NaCl, 2 $MgCl_2$, 10 HEPES, 0.5 EGTA, 2 Mg-ATP, 0.3 Na-GTP, 5 D-glucose, 20 disodium phosphocreatine (pH 7.2 with KOH, liquid junction potential of 12 mV). ChR2 was activated by a sapphire 488-nm laser (75 mW maximum output power, Coherent)[46]. Offline analysis was performed using Pulse and Igor Pro software.

Statistical analyses.

All results are presented as mean ± s.e.m. and were analyzed by the commercially available GraphPad Prism 7 software (GraphPad Inc.). Statistical significance was defined as $P < 0.05$. Normality and equality of variance were analyzed with the D′Agostino-Pearson omnibus test and Bartlett's test, respectively. In cases where sample sizes were too small, data distribution was assumed to be normal. Based on the results of these tests, appropriate parametric (two-tailed unpaired *t*-test) or non-parametric (Mann-Whitney *U* test) tests were performed. Time-dependent measures assessed during microdialysis, fear conditioning and optogenetic experiments were analyzed with repeated-measures ANOVA followed by Bonferroni post hoc analysis. No statistical methods were used to predetermine sample sizes. Sample sizes were based on those reported in previous publications[1,4,37,38,47–50]. Animals were randomly allocated into different experimental groups. Conditional knockout mice and control littermates were assigned to the experimental group on the basis of genotype. No specific randomization method was used. Age-matched littermates were used as controls in all experiments. For behavioral analysis, experimenters were blind to experimental conditions. Injection sites and viral expression were confirmed for all animals by experimenters blind to behavioral results. Mice showing incorrect cannula placement, injection sites or optic fiber placement were excluded from analysis by experimenters blind to treatment.

Reporting Summary.

Further information on experimental design is available in the Nature Research Reporting Summary linked to this article.

Data and code availability.

The data that support the findings of this study are available from the corresponding author upon reasonable request. No custom or open source code was used for data collection and analyses.

Supplementary Material

Refer to Web version on PubMed Central for supplementary material.

Acknowledgements

We thank S. Bauer, C. Eggert, D. Harbich, M. Holzapfel, R. Huttl, A. Mederer, A. Parl, A. Ressle, R. Stoffel, L. Tietze and S. Unkmeir for excellent technical support, M. Eder for Core Unit infrastructure and J. Keverne for manuscript proofreading. This work was partially supported by the Max Planck Society, Volkswagen Foundation, German Federal Ministry of Education and Research (FKZ:01ZX1314H to J.M.D., W.W.), Helmholtz Alliance ICEMED (to W.W), Chica and Heinz Schaller Foundation (to V.G.), DFG (SFB 1134 to V.G.) and FAPESP (2013/03445-3 to K.S.G.).

References

1. Refojo D et al. Science 333, 1903–1907 (2011). [PubMed: 21885734]
2. Swanson LW, Sawchenko PE, Rivier J & Vale WW Neuroendocrinology 36, 165–186 (1983). [PubMed: 6601247]

3. Henckens MJAG, Deussing JM & Chen A Nat. Rev. Neurosci 17, 636–651 (2016). [PubMed: 27586075]
4. Lemos JC et al. Nature 490, 402–406 (2012). [PubMed: 22992525]
5. Grieder TE et al. Nat. Neurosci 17, 1751–1758 (2014). [PubMed: 25402857]
6. Silberman Y & Winder DG Front. Psychiatry 4, 42 (2013). [PubMed: 23755023]
7. Wanat MJ, Bonci A & Phillips PE M. Nat. Neurosci 16, 383–385 (2013).
8. George O, Le Moal M & Koob GF Physiol. Behav 106, 58–64 (2012). [PubMed: 22108506]
9. Sanford CA et al. Neuron 93, 164–178 (2017). [PubMed: 28017470]
10. Haubensak W et al. Nature 468, 270–276 (2010). [PubMed: 21068836]
11. Jennings JH et al. Nature 496, 224–228 (2013). [PubMed: 23515155]
12. Fadok JP et al. Nature 542, 96–100 (2017). [PubMed: 28117439]
13. Rodaros D, Caruana DA, Amir S & Stewart J Neuroscience 150, 8–13 (2007). [PubMed: 17961928]
14. Tagliaferro P & Morales MJ Comp. Neurol 506, 616–626 (2008).
15. Kubota Y Curr. Opin. Neurobiol 26, 7–14 (2014). [PubMed: 24650498]
16. Yan X, Toth Z, Schultz L, Ribak CE & Baram TZ 243, 231–243 (1998).
17. Robison AJ Trends Neurosci 37, 653–662 (2014). [PubMed: 25087161]
18. Robison AJ et al. J. Neurosci 33, 4295–4307 (2013). [PubMed: 23467346]
19. Wanat MJ, Hopf FW, Stuber GD, Phillips PEM & Bonci AJ Physiol. (Lond.) 586, 2157–2170 (2008).
20. Garcia I et al. Dev. Cell 30, 645–659 (2014). [PubMed: 25199688]
21. Taniguchi H et al. Neuron 71, 995–1013 (2011). [PubMed: 21943598]
22. Madisen L et al. Nat. Neurosci 15, 793–802 (2012). [PubMed: 22446880]
23. Goebbels S et al. Genesis 44, 611–621 (2006). [PubMed: 17146780]
24. Erdmann G, Schütz G & Berger S BMC Neurosci 8, 63 (2007). [PubMed: 17683525]
25. Brust RD, Corcoran AE, Richerson GB, Nattie E & Dymecki SM Cell Reports 9, 2152–2165 (2014). [PubMed: 25497093]
26. Bang SJ, Jensen P, Dymecki SM & Commons KG Eur. J. Neurosci 35, 85–96 (2012). [PubMed: 22151329]
27. Miyoshi G et al. J. Neurosci 30, 1582–1594 (2010). [PubMed: 20130169]
28. Kühne C et al. J. Comp. Neurol 520, 3150–3180 (2012). [PubMed: 22886732]
29. Rodríguez CI et al. Nat. Genet 25, 139–140 (2000). [PubMed: 10835623]
30. Farley FW, Soriano P, Steffen LS & Dymecki SM Genesis 28, 106–110 (2000). [PubMed: 11105051]
31. Grinevich V, Brecht M & Osten PJ Neurosci. 25, 8250–8258 (2005).
32. Pilpel N, Landeck N, Klugmann M, Seeburg PH & Schwarz MK J. Neurosci. Methods 182, 55–63 (2009). [PubMed: 19505498]
33. Nielsen SM, Nielsen LZ, Hjorth SA, Perrin MH & Vale WW Proc. Natl Acad. Sci. USA 97, 10277–10281 (2000). [PubMed: 10963687]
34. Anderzhanova EA et al. Eur. J. Pharmacol 708, 95–104 (2013). [PubMed: 23524098]
35. Chen Y, Molet J, Gunn BG, Ressler K & Baram TZ Endocrinology 156, 4769–4780 (2015). [PubMed: 26402844]
36. Muglia L, Jacobson L, Dikkes P & Majzoub JA Nature 373, 427–432 (1995). [PubMed: 7830793]
37. Dedic N et al. Mol. Psychiatry 23, 533–543 (2018). [PubMed: 28696432]
38. Hartmann J et al. Mol. Psychiatry 22, 466–475 (2017). [PubMed: 27240530]
39. Kamprath K & Wotjak CT Learn. Mem 11, 770–786 (2004). [PubMed: 15537742]
40. Siegmund A, Langnaese K & Wotjak CT Behav. Brain Res 157, 291–298 (2005). [PubMed: 15639180]
41. Thoeringer CK et al. Genes Brain Behav. 9, 947–957 (2010). [PubMed: 20659172]
42. Kamprath K et al. J. Neurosci 26, 6677–6686 (2006). [PubMed: 16793875]

43. Kamprath K et al. Genes Brain Behav. 8, 203–211 (2009). [PubMed: 19077175]
44. Siegmund A & Wotjak CT J. Psychiatr. Res 41, 848–860 (2007). [PubMed: 17027033]
45. Siegmund A et al. J. Psychiatr. Res 43, 1156–1165 (2009). [PubMed: 19304295]
46. Dine J et al. Front. Cell. Neurosci 10, 108 (2016). [PubMed: 27199662]
47. Vogl AM et al. Nat. Neurosci 18, 239–251 (2015). [PubMed: 25581363]
48. Wang XD et al. Nat. Neurosci 16, 706–713 (2013). [PubMed: 23644483]
49. Walsh JJ et al. Nat. Neurosci 17, 27–29 (2014). [PubMed: 24270188]
50. Pomrenze MB et al. Front. Neurosci 9, 487 (2015). [PubMed: 26733798]

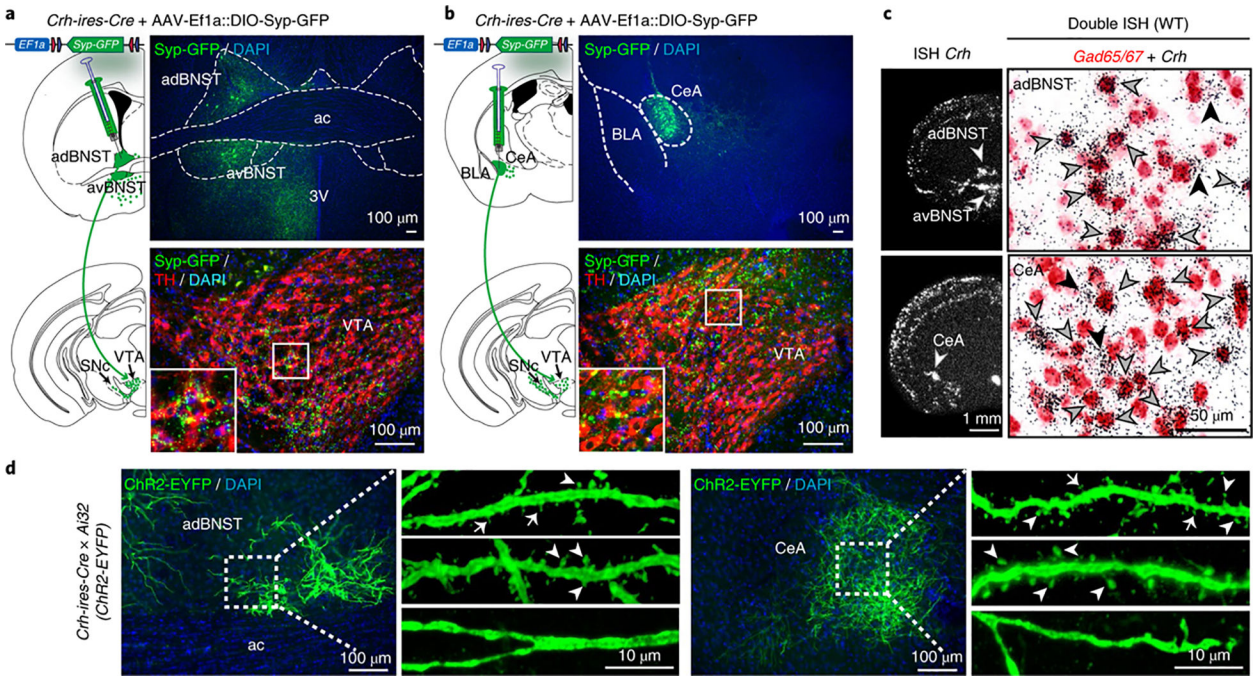

Fig. 1 |. GABAergic CRH neurons in the aBNST and CeA project to the VTA and carry dendritic spines.

a,b, Syp-GFP in the aBNST and CeA (top) and projections in the VTA (bottom) in *Crh-ires-Cre* mice; TH, dopaminergic marker tyrosine hydroxylase. **c**, *Crh* mRNA expression determined by in situ hybridization (ISH, left). Double ISH (brightfield, right): *Crh* (silver grains) is primarily expressed in GABAergic neurons (*Gad65/67*-positive, red staining) of the adBNST and CeA. Black arrowheads, *Crh*-positive; gray arrowheads, *Gad65/67*- and *Crh*-positive. Quantification in Supplementary Fig. 3. **d**, Spiny and aspiny CRH neurons in the aBNST and CeA of *Crh-ires-Cre;Ai32(ChR2-EYFP)* mice. Thin spines, arrows; mushroom-like spines, arrowheads. Experiments in **a-c** and **d** were independently replicated three and four times, respectively. Anterior commissure, ac; anterior dorsal BNST, adBNST; anterior ventral BNST, avBNST; third ventricle, 3 V; basolateral amygdala, BLA.

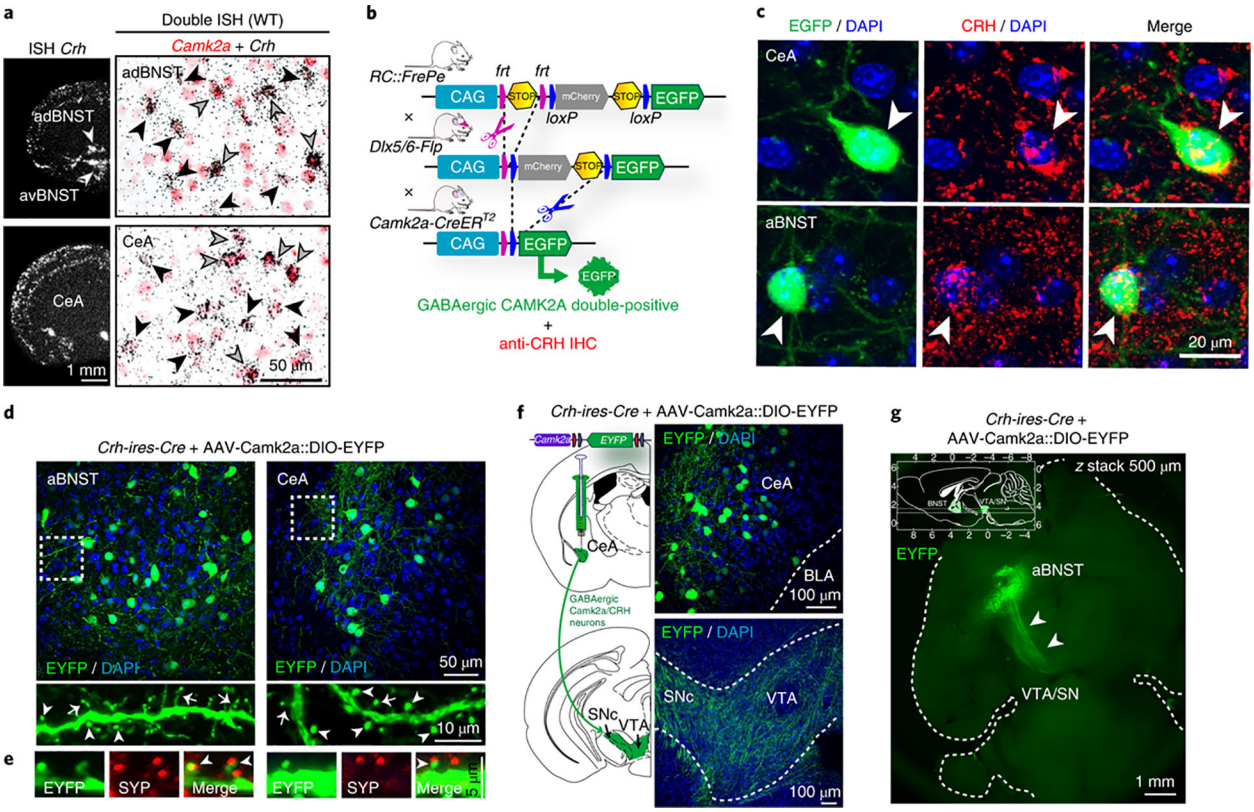

Fig. 2 |. VTA-projecting spiny GABAergic CRH neurons express *Camk2a*.

a, *Crh* mRNA expression determined by in situ hybridization (ISH, left). Double ISH (right) shows that a subset of *Crh* neurons in the adBNST and CeA coexpress *Camk2a*. Black arrowheads, *Crh*-positive; gray arrowheads, *Camk2a* and *Crh* double positive. Quantifications in Supplementary Fig. 3. **b**, Schematic representation of dual fate mapping strategy. IHC, immunohistochemistry. **c**, Representative sections of *RC::FrePe;Dlx5/6-Flp;Camk2a-CreER*^{T2} mice (dual-recombinase-responsive fluorescent reporter mice expressing *Dlx5/6-Flpe* and *Camk2a-CreERT2)* and subsequent CRH immunostaining (red) show triple-positive GABAergic CAMK2A CRH neurons (arrowheads) in the CeA and aBNST. **d,e**, CAMK2A CRH neurons carry thin (arrows) and mushroom-like (arrowheads) spines (**d**), which receive presynaptic input determined by synaptophysin (SYP, red) immunostaining (**e**). **f**, CeA CAMK2A CRH neurons (top) and VTA-innervating fibers (bottom). **g**, Whole brain CLARITY: horizontal *z*-stack image shows GABAergic, CAMK2A- and CRH-positive aBNST-VTA projections (arrowheads); see Supplementary Video 1. Inset shows stack range, delimited by horizontal lines; axes in millimeters, with bregma at 0 mm on the top and right axes and interaural line at 0 mm at the bottom and left axes. All experiments were independently replicated three times. Anterior dorsal BNST, adBNST; anterior ventral BNST, avBNST; basolateral amygdala, BLA.

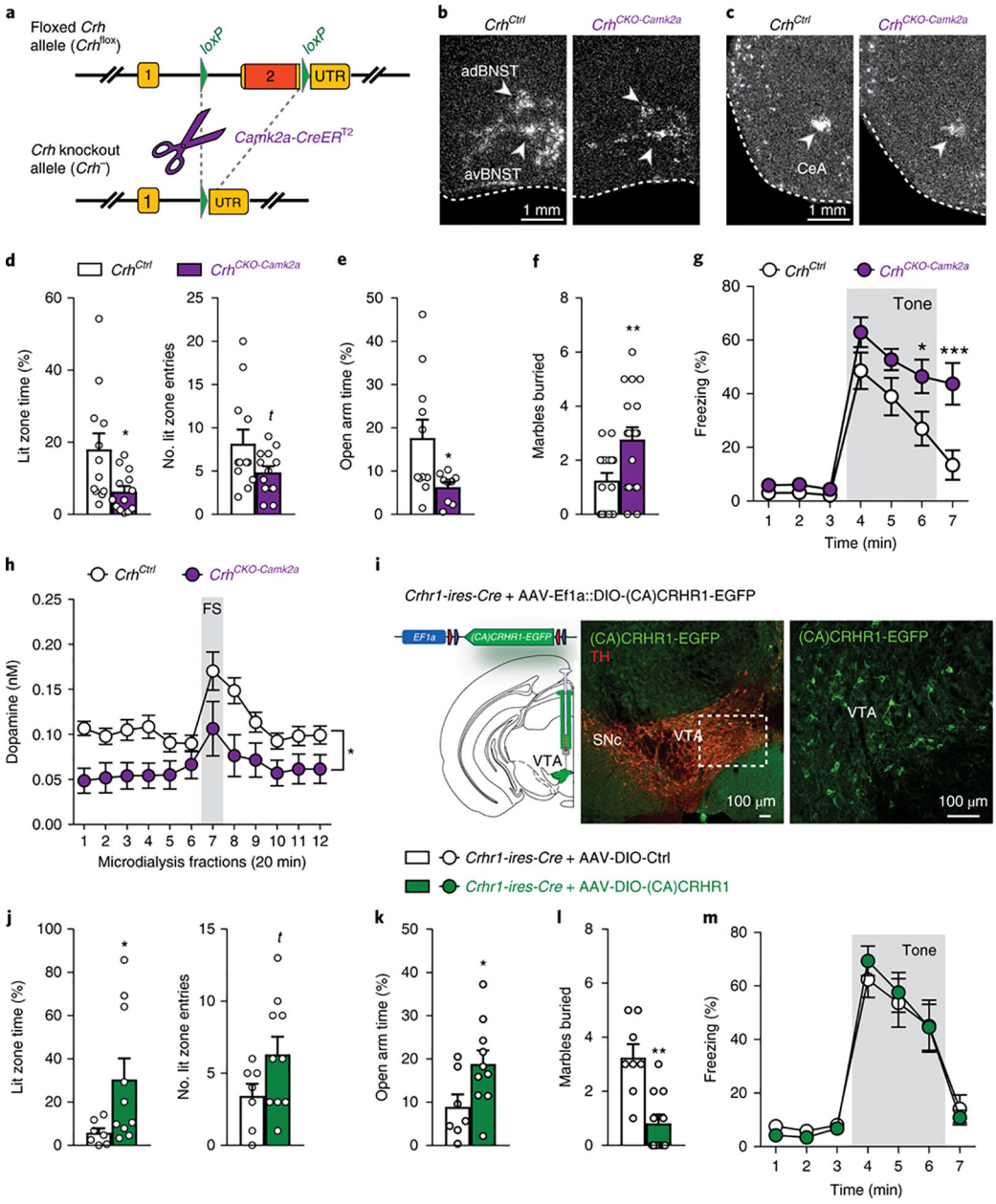

Fig. 3 |. CRH in CAMK2A neurons regulates anxiety, fear memory expression and dopamine release in the prefrontal cortex.

a, Schematic illustration of the targeted *Crh* allele (*Crh*^{flox}); details in Supplementary Fig. 7; UTR, untranslated region. **b**, **c**, In situ hybridization showing *Crh* mRNA deletion pattern in *Crh*$^{CKO\text{-}Camk2a}$ mice; quantifications from four independent experiments in Supplementary Fig. 8b. **d**, Dark-light box test: lit zone time ($t_{(23)}$ = 2.6, **P* = 0.018) and lit entries ($t_{(23)}$ = 1.9, *P* = 0.068); unpaired two-tailed *t*-test, *n* = 12 *Crh*^{Ctrl}, 13 *Crh*$^{CKO\text{-}Camk2a}$. **e**, Open arm time (%) in the EPM ($t_{(18)}$ = 2.4, *P*= 0.031; unpaired two-tailed *t*-test, *n* = 11 *Crh*^{Ctrl}, 9 *Crh*$^{CKO\text{-}Camk2a}$). **f**, Marble burying test ($t_{(31)}$ = 2.8, ***P* = 0.009; unpaired two-tailed *t*-test, *n* = 16 *Crh*^{Ctrl}, 17 *Crh*$^{CKO\text{-}Camk2a}$). **g**, Cued fear conditioning (repeated-measures ANOVA time × group interaction: $F_{(6156)}$ = 3.88, *P* = 0.0012; Bonferroni post hoc test, * *P*<0.05,

***P< 0.0001; n = 13 Crh^{Ctrl}, 15 $Crh^{CKO<amk2a}$). **h**, In vivo microdialysis showing decreased dopamine release in the prefrontal cortex of $Crh^{CKO\text{-}Camk2a}$ mice under baseline conditions and following footshock (FS) stress (repeated-measures ANOVA genotype effect: $F_{(117)}$ = 7.14, * P = 0.02; n = 10 Crh^{Ctrl}, 9 $Crh^{CKO\text{-}Camk2a}$). i, Cre-dependent expression of a constitutively active CRHR1-EGFP fusion construct (AAV-Ef1a::DIO-(CA)CRHR1-EGFP) in VTA neurons of *Crhr1-ires-Cre* mice (representative images from three independent experiments; details in Supplementary Figs. 11 and 12). Littermate controls were injected with AAV-Ef1a::DIO-mCherry. **j-m**, *Crhr1-ires-Cre* mice expressing (CA)CRHR1 in the VTA exhibit decreased anxiety in the dark-light box test (**j**; lit zone time: U = 14, *P= 0.043; lit zone entries: U = 20, P= 0.1; Mann-Whitney U test two-tailed; n = 7 Ctrl, 10 (CA)CRHR1), EPM (**k**; $t_{(15)}$ = 2.2, *P= 0.043; unpaired two-tailed t-test; n = 7 Ctrl, 10 (CA)CRHR1) and marble burying test (**l**; $t_{(17)}$ = 4.3, ***P = 0.005; unpaired two-tailed t-test; n = 8 Ctrl, 11 (CA) CRHR1) without showing alterations in cued fear conditioning (**m**; repeated-measures ANOVA time × group interaction: $F_{(6102)}$ = 0.45, P = 0.84; n = 8 *Ctrl*, 11 (CA)CRHR1). Anterior dorsal BNST, adBNST; anterior ventral BNST, avBNST; tyrosine hydroxylase, TH. Error bars represent s.e.m.